Materials Research Proceedings 41 (2024) 2607-2616 https://doi.org/10.21741/9781644903131-286

Effect of different auxetic cell design on the compression behavior of FDMed structures

NAPOLITANO Francesco[1,a *], CARDENIO Ivano[2,b], DEFINA Filippo[3,c], MANCO Emanuele[2,d], MANZO Alessandro[3,e], PAPA Ilaria[1,2,f] and RUSSO Pietro[1,g]

[1]Institute of Polymers, Composites and Biomaterials, National Research Council, Via Campi Flegrei 34, 80078, Pozzuoli, Naples, Italy

[2]Department of Chemical, Materials and Industrial Production Engineering, University of Naples "Federico II", P.leTecchio 80, 80125, Naples, Italy

[3]3DnA srl, Consorzio "il Sole", Viale Impero, 80038 Pomigliano D'arco, Naples, Italy

[a]francesco.napolitano@ipcb.cnr.it, [b]cardenioivano@gmail.com, [c]filippo.defina@3dnasrl.it, [d]emanuele.manco@unina.it, [e]alessandro.manzo@3dnasrl.it, [f]ilaria.papa@unina.it, [g]pietro.russo@ipcb.cnr.it

Keywords: Auxetic, Cellular Structures, Compression, Thermoplastic, FDM

Abstract. Among the different additive manufacturing technologies for polymeric materials, Fused Deposition Modelling has obtained great visibility and, thanks to the numerous studies on the process conditions, reached high quality of workpiece production. Nevertheless, the slicers are projected to replicate standard and easy to reproduce patterns, which don't take into account the final use of the workpiece produced. An optimization of the extruded material is represented by the design oriented to support specific loads, which are applied along specific directions. In this research work is proposed the use of auxetic geometry and two different cell types are proposed and compared with the related conventional workpieces, printed with the same volume density. The use of auxetic design allows for differentiation of the load-bearing and to obtain structures which don't lose their original shape and that can adsorb the compressive energy reaching the compaction which improves the final resistance.

Introduction

Sandwich structure composites consist of two rigid faces to resist external loads and an embedded cell core to increase the moment of inertia. Due to their high specific modulus and strength, they find applications in many fields, such as aerospace, automotive, marine and energy industries [1]. For this type of composite, the specific core architecture offers greater flexibility in tailoring their ultimate performance and, in this frame, particular interest is focused on auxetic structures [2,3]. Auxetic materials are characterized by a negative Poisson's ratio, the immediate effect of which is to allow a behaviour opposite to that found in classical structural materials; that is, when subjected to tensile stress they tend to increase their transverse dimension, while, if compressed, they tend to shrink transversely. [4,5]. An unexpected behaviour also occurs in bending where a material with auxetic behaviour tends to rise in the central area, conforming adequately to the curvature. The naturally auxetic materials are single crystals of arsenic [6] and cadmium [7], α-cristobalite [8], iron pyrites [9], and many cubic elemental metals [10]. Other examples regard biological materials, such as cat skin [11], salamander skin [12], cow teat skin [13], and load-bearing cancellous bone from human shins [14].

Studying the structures of these natural materials, in the late 1980s the researchers tried to replicate them to obtain auxetic structures from non-auxetic materials: an early example was an auxetic polyurethane foam [15,16].

The way to obtain an auxetic behaviour, from a conventional material, is to assemble a cellular structure in which each cell reproduces the load adsorption in the same manner as an auxetic material [17]. The elementary cells that constitute the basic structure of most auxetic materials can have different shapes of which it is possible, with trigonometric formulas, to calculate the rotation of the individual walls of each cell in relation to the load applied and therefore to have an idea of how to more accurately predict the overall mechanical behaviour of the structure. Over the years, some research studies were proposed with various geometries of the cells, aimed at achieving auxetic behaviour in cellular structures. The most simple to be designed, and the most adopted in the early stage of the research, is the hexagon concave [18–21], and its auxetic properties are demonstrated by finite elements analysis [22]. For these reasons, it was decided to design different cells to be tested in this experimental study.

The study of auxetic structures is relatively recent [15], but the advantages of this cell architecture are now completely undeniable [23]. The potential and real applications of auxetic materials are rapidly increasing, but their diffusion sometimes seems hindered by the fact that this is a new research sector and the phenomena are not always very clear or in any case not always describable with mathematical formulas easy to use. Furthermore, production costs are very high, the creation of the cells is complex and it is therefore preferable to use traditional materials even if they have lower performance. Thanks to the customization given by 3D printing techniques, such as the Fused Deposition Modelling one (FDM), the design of auxetic cells is rapidly increasing in metallic and polymeric materials. This manufacturing approach allows for improved resistance under impact and compression strength [24].

3D printing offers a considerable number of advantages, the most significant of which is the ability to produce highly complex designs that would otherwise be impossible to create quickly, reducing waste of material and time for post-process machining while also offering many possibilities of 3D printing.

The contribution of the cellular structure could be improved through the choice of a properly reinforced polymer or polymeric blend which allows to performance of the expected response under a specific load. Furthermore, the cellular auxetic structures aid in managing the displacement of the singular cell element by driving the load transmission along the thicker and most resistant elements. If compared with a conventional 3D printed item, these new structures, having the same volume density, are characterized by an increased resistance given that the conventional FDM printing patterns are focused on the simple volume filling and not on the strategic filling.

In this frame, the work aims to design a reinforced polymer giving the best response under the expected load. An appropriate cell architecture will be chosen which ensures the best performances under compression load. The samples will be produced by the FDM process and, simultaneously, other samples will be produced by using traditional infill strategy to achieve the same volumetric density. All the structures will be tested under compression. The damaged samples were finally inspected.

Materials and methods

Core design

The in-plane behaviour of lattice composites is strongly affected by the core structure [25]. Here, two types of core topologies are considered. The main purpose of this work is to identify the cell deformation pattern and investigate how they affect compressive performances. Two types of cellular structures are fixed to have the same dimension as the unit cell. This approach provides a more straightforward observation of the divergent unit cell deformation pattern.

Gibson and Ashby proposed a numerical model to simplify the estimation of elemental cell behaviour and is based on the cell design in Figure 1 [26].

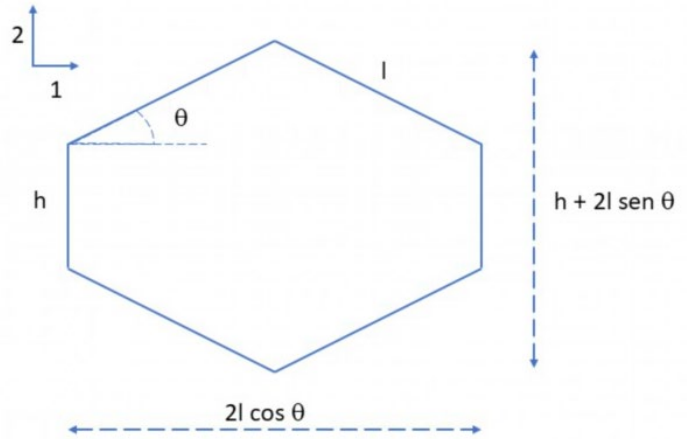

Figure 1. Design and dimensions of the elemental cell.

This cell could be loaded in direction 1, and in this case, the load is perpendicular to the vertical elements h which are also the most resistant. So the best loading direction is represented by direction 2, in this case, the load is parallel to the elements h which allows for improved cell resistance and is aided by the elements l which distribute the load on both sides. By considering the loading direction 2, the cell has two collapsing behaviour. The first one is the elastic buckling: in this case, the vertical elements h reach the instability before the fracture; the second one is the plastic collapse, in which case the rupture of the vertical elements causes the cell failure.

$$(\sigma_{el})_2 = \frac{n^2\pi^2}{24} E_s \frac{(t/l)^3}{(h/l)^2 \cos\theta} \quad (1)$$

$$(\sigma_{pl})_2 = \sigma_{ys} \left(\frac{t}{l}\right)^2 \frac{1}{2\cos^2\theta} \quad (2)$$

The predominant failure mode is subjected to the maximum value which can reach the ratio between the thickness of the cell walls and the length of inclined elements. This ratio is:

$$(t/l)_{critical} = \frac{12\,(h/l)^2}{n^2\pi^2 \cos\theta} \left(\frac{\sigma_{ys}}{E_s}\right) \quad (3)$$

Where

E_s : elastic modulus of the cell material

σ_{ys} : yield strength of the cell material

t : thickness of the cell elements h and l

n is a shape factor obtained from the ratio between vertical elements and inclined elements (Table 1).

Table 1. Shape factor n for different h/l ratios.

h/l	n
1	0.686
1.5	0.760
2	0.860

Core design selection

The first step for the selection of the cells constituting the core of the structures under examination is to appropriately take the geometric relationships for the construction of the elementary cells necessary for the construction of the specimens of the experimental plan.

The values taken into consideration are reported in the table 2.

Table 2. Dimensions of the designed core topology

Angle	t/l	h/l	t [mm]	l [mm]	h [mm]
-30°	0.4000	1.8500	1	2.5	8.000
-45°	0.3100	2.0849	1	3.226	6.726

Cell (-45°)

The elementary cell at -45 ° was designed starting from the geometric parameters generated by the numerical model and was dimensioned by defining the measurement of "l", of the first angle of 45° and of the thickness "t". The other measures were quoted based on the latter.

The dimensions were assigned to the average line defined as the construction line and then created an internal and external offset of 0.5 mm each respectively.

For compression sample construction, the sketch was subsequently extruded with a height of 30 mm. The constructed cell has a length of l=12.535mm, a width of L=3.0mm and a Volume factor of V_f=0.449 as shown in Figure 2 a), in Figure 2 b) is reported a three dimensional example of single cell extrusion.

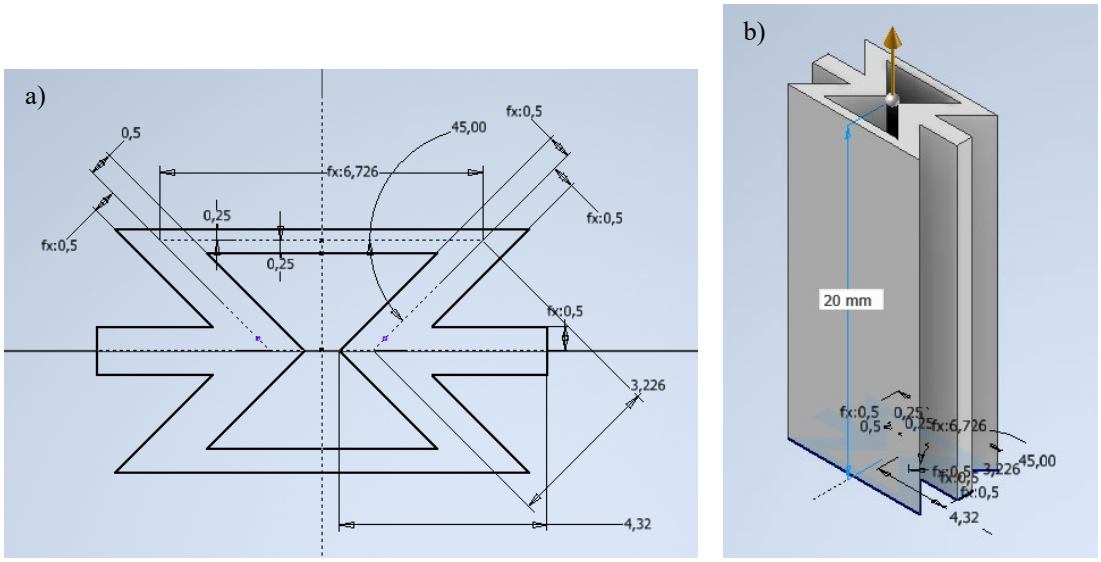

Figure 2. Model of Cell (-45°): a) CAD model; b) extruded cell.

Cell (-30°)

For comparison with the -45° cell, a free h parameter was chosen for the -30° cell. The construction phase instead followed the logic of the previous cell and an extrusion always for a height of 30mm in accordance with sample design for compression tests.

The constructed cell has a length of l=9.390 mm, a width of L=5.062 mm and a Volume factor of V_f=0.552 as shown in Figure 3 a), in Figure 3 b) is reported a three dimensional example of single cell extrusion.

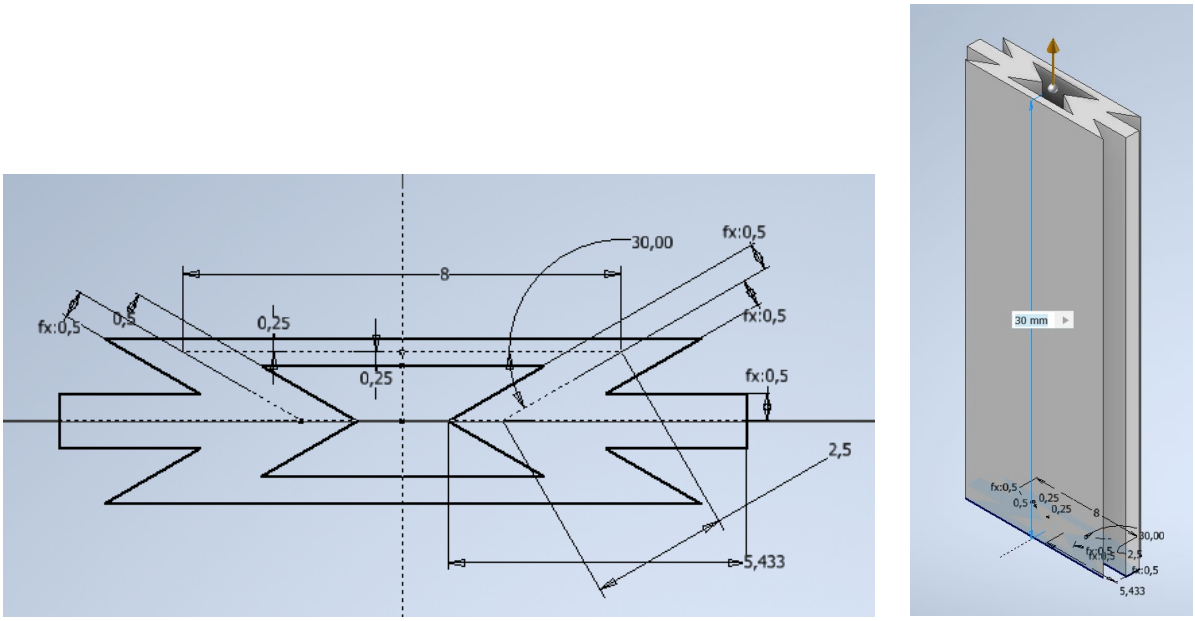

Figure 3. Model of Cell (-30°): a) CAD model; b) extruded cell.

Samples design

The dimensions of the compression specimens were established according to the standard ASTM C365 [27].

In particular, three specimens for each design were produced: they have 30 mm x 30 mm x 30 mm dimensions. Four different sample designs were proposed, two auxetic and two traditional. Regarding the auxetic, the first one corresponds to the auxetic cell with θ = -30° and is named A-30, the second one corresponds to the auxetic cell with θ = -45° and is named A-45. The number of cell repetitions (n_r) to be carried out for each specimen was evaluated with the following formula:

$$nr = \frac{Ws/ls}{l/W} \quad (4)$$

Where W and Ws are the cell and sample width, respectively, while l and ls are the cell and sample length.

To evaluate the effect of the auxetic structure on the mechanical performance, two traditional designs for comparison specimens were produced, they have the same dimensions and a filling infill equal to the volume factor, V_f, of the auxetic cells. For the infill strategy, the chosen pattern is +/- 45°, with different volume factor which is aimed to reproduce the same as auxetic. Fig. 5 a and b show respectively the infill strategy for the traditional which corresponds to auxetic 30° and 45°.

So, for the cell -30° an n_r=2.39 for both x and z directions were established and for the cell -45° an n_r =5.93 and n_r=3.19 were selected for x and z directions respectively (Figure 4).

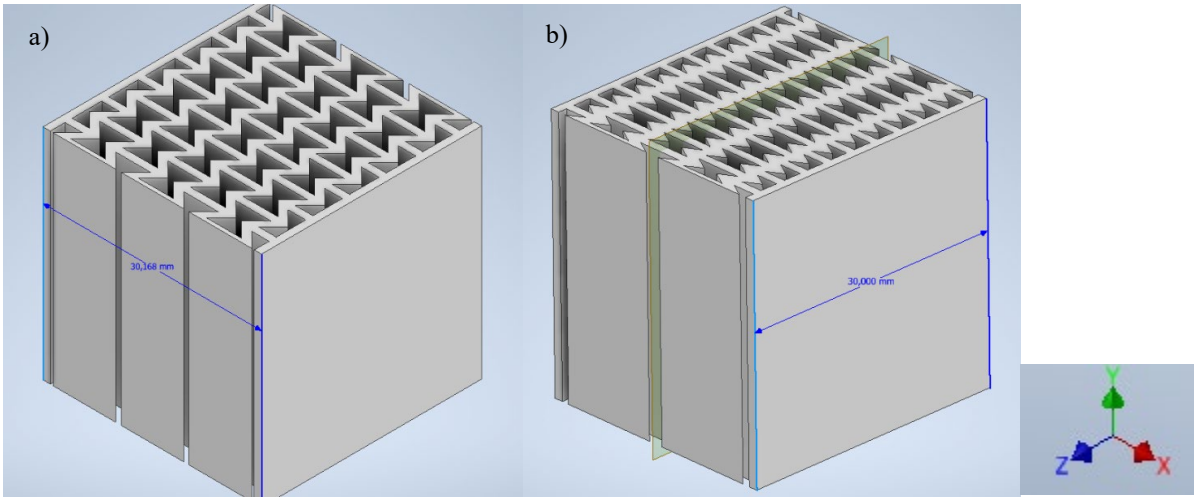

Figure 4. Compression samples: a) A-45; b) A-30°.

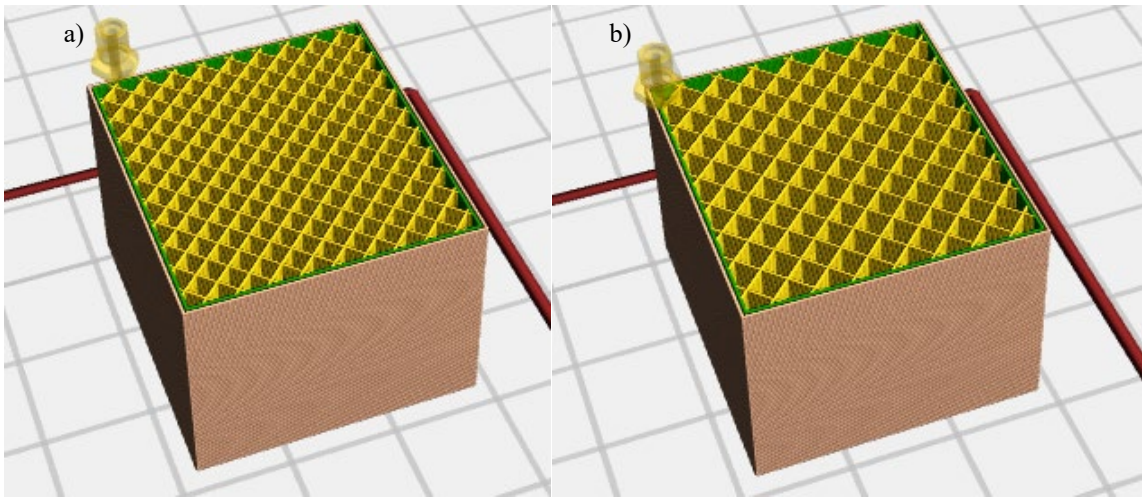

Figure 5. Infill strategy of the traditional compression samples.

The material used is a commercial PLA black by Flashforge and the samples were produced by Flashforge 3D printer at 3DNa srl in Naples with a build volume equal to 300 × 270 × 200 mm was used. The extruders move along the x and y axes, while the print bed moves along the z axis. The process starts by uploading the STL file into the related software FlashPrint. It is possible to set process parameters such as materials, deposition strategy; printing speed and temperature are set as optimal according to the material (Table 3).

Table 3. Printer parameters selected.

Extruder Temperature [°C]	220
Plate Temperature [°C]	55
Layer height [mm]	0.2
Print speed [mm/s]	300

Sample characterization

Compression tests were performed using an Instron mod. 4505, equipped with a 100kN load cell and having a crosshead speed 2 mm/min.

Results and discussion

The following Table 4 shows the average and the standard deviation for the traditional specimens. Table 5 summarizes the average and standard deviation values for the auxetic specimens. Figure 6 shows the four representative curves of the compression test, each referring to one different sample design. The process of compression of the serrations of auxetic 3D structures shows a nature related to the characteristics of the destruction of the structures. Once the critical deformation is reached, the brittle material fractures and initially splits into several large parts and the stress drops to almost zero. Going to increase the deformation of the fragments obtained, a packing phenomenon is obtained, the stress increases slightly, which leads to the further fracture of large parts and the formation of smaller ones, then the process is repeated. Such a cracking mechanism leads to the formation of serrations on the load curve. The envelope of this curve also indicates the presence of a pronounced plateau. The area under this curve characterizes the adsorbed strain energy. This phenomenon was just recorded in [28].

Table 4. Average and the standard deviation for the traditional specimens.

Sample	Max stress [MPa]	Young's modulus [MPa]
T -30	24.95 ± 0.44	860.77 ± 2.47
T -45	19.95 ± 1.68	742.36 ± 2.67

Table 5. Average and the standard deviation values for the auxetic specimens.

Sample	Max stress 1 [MPa]	Young's modulus 1 [MPa]	Max stress 2 [MPa]	Young's modulus 2 [MPa]	Max stress 3 [MPa]	Young's modulus 3 [MPa]
A -30	14.98 ± 0.36	624.89 ± 11.23	12.96 ± 1.75	383.71 ± 85.06	14.95 ± 1.29	273.44 ± 14.99
A -45	7.36 ± 0.44	259.93 ± 18.99	7.20 ± 1.01	127.37 ± 31.44	7.51 ± 2.16	160.44 ± 50.12

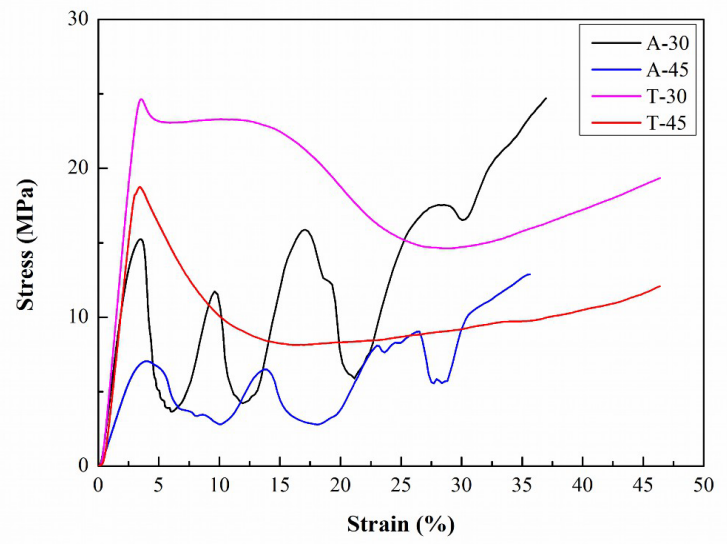

Figure 6. Curves of the compression test comparison.

Table 6 reports the results regarding the elastic springback and the shape ratio of the tested samples. The elastic springback is evaluated by considering the ratio between the final height of the sample, under the applied compression load, and the height of the sample after the load release.

The shape ratio is evaluated by considering the ratio between the final in-plane dimensions of the sample and the initial dimensions. It is reported a significant reduction in the shape ratio between traditional samples and auxetic ones.

Table 6. Elastic spring back and the shape ratio of the tested samples.

Sample	Elastic spring back	Shape ratio
T-30	1.35 ± 0.03	1.35 ± 0.08
T-45	1.15 ± 0.06	1.30 ± 0.07
A-30	1.15 ± 0.01	1.12 ± 0.12
A-45	1.14 ± 0.01	1.10 ± 0.11

From these preliminary tests, the following conclusions can be drawn:

- The cell design procedure leads to structures which can be obtained through a standard FDM process.
- The structure resistance mainly depends on the volume density of the workpiece and is not dependent on the thickness of the vertical elements.
- Auxetic structures show a series of peaks, in the compression tests, corresponding to the number of cell lines under the load direction.
- Although the max stress value of the auxetic structures is lower than the traditional ones, they continue to bear the collapse and report almost the same values for each element collapsing. This behaviour is also reported in other research work [28].
- After the compression peak is reached, the mechanism of resistance is completely different. The increase in the strength value for the traditional samples is due to the influence of the testing metal plates; on the other hand, the increase in the auxetic structure is due to a major compaction of the whole structure. This is evident from the shape ratio.
- The influence of the auxetic geometry is evident in the reduction of the shape ratio. This value shows a decrease between 15% and 17% in auxetic samples compared to traditional ones.
- More tests are useful to validate the cell design and the advantages against the traditional printing infill.

This study is a preliminary analysis for a more complete future work where, following a complete characterization of the different auxetic structures, the authors will try to propose a numerical model from which it is possible to evaluate the most appropriate cell to obtain the desired mechanical performances.

References

[1] V. Birman, G.A. Kardomateas, Review of current trends in research and applications of sandwich structures, Compos. Part B Eng. 142 (2018). https://doi.org/10.1016/j.compositesb.2018.01.027

[2] C. Yang, H.D. Vora, Y. Chang, Behavior of auxetic structures under compression and impact forces, Smart Mater. Struct. 27 (2018). https://doi.org/10.1088/1361-665X/aaa3cf

[3] O. Duncan, T. Shepherd, C. Moroney, L. Foster, P.D. Venkatraman, K. Winwood, T. Allen, A. Alderson, Review of auxetic materials for sports applications: Expanding options in comfort and protection, Appl. Sci. 8 (2018). https://doi.org/10.3390/app8060941

[4] T. Li, Y. Chen, X. Hu, Y. Li, L. Wang, Exploiting negative Poisson's ratio to design 3D-printed composites with enhanced mechanical properties, Mater. Des. 142 (2018). https://doi.org/10.1016/j.matdes.2018.01.034

[5] K.E. Evans, A. Alderson, Auxetic materials: Functional materials and structures from lateral thinking!, Adv. Mater. 12 (2000). https://doi.org/10.1002/(SICI)1521-4095(200005)12:9<617::AID-ADMA617>3.0.CO;2-3

[6] D.J. Gunton, G.A. Saunders, The Young's modulus and Poisson's ratio of arsenic, antimony and bismuth, J. Mater. Sci. 7 (1972). https://doi.org/10.1007/BF00550070

[7] Y. Li, The anisotropic behavior of Poisson's ratio, Young's modulus, and shear modulus in hexagonal materials, Phys. Status Solidi 38 (1976). https://doi.org/10.1002/pssa.2210380119

[8] A. Yeganeh-Haeri, D.J. Weidner, J.B. Parise, Elasticity of α-cristobalite: A silicon dioxide with a negative poisson's ratio, Science (80-.). 257 (1992). https://doi.org/10.1126/science.257.5070.650

[9] L.N.G. F., A Treatise on the Mathematical Theory of Elasticity, Nature 105 (1920). https://doi.org/10.1038/105511a0

[10] R.H. Baughman, J.M. Shacklette, A.A. Zakhidov, S. Stafström, Negative poisson's ratios as a common feature of cubic metals, Nature 392 (1998). https://doi.org/10.1038/32842

[11] D.R. Veronda, R.A. Westmann, Mechanical characterization of skin-Finite deformations, J. Biomech. 3 (1970). https://doi.org/10.1016/0021-9290(70)90055-2

[12] L.M. Frolich, M. LaBarbera, W.P. Stevens, Poisson's ratio of a crossed fibre sheath: the skin of aquatic salamanders, J. Zool. 232 (1994). https://doi.org/10.1111/j.1469-7998.1994.tb01571.x

[13] C. Lees, J.F.V. Vincent, J.E. Hillerton, Poisson's ratio in skin, Biomed. Mater. Eng. 1 (1991). https://doi.org/10.3233/BME-1991-1104

[14] J.L. Williams, J.L. Lewis, Properties and an anisotropic model of cancellous bone from the proximal tibial epiphysis, J. Biomech. Eng. 104 (1982). https://doi.org/10.1115/1.3138303

[15] R. Lakes, Foam structures with a negative poisson's ratio, Science (80-.). 235 (1987). https://doi.org/10.1126/science.235.4792.1038

[16] A. Alderson, K.L. Alderson, Auxetic materials, Proc. Inst. Mech. Eng. Part G J. Aerosp. Eng. 221 (2007) 565–575. https://doi.org/10.1243/09544100JAERO185

[17] H.S. Gill, Mechanical and structure properties of cellular auxetic materials, in: Mater. Today Proc., 2020.

[18] An isotropic three-dimensional structure with Poisson's ratio =-1, J. Elast. 15 (1985). https://doi.org/10.1007/BF00042531

[19] A.G. Kolpakov, Determination of the average characteristics of elastic frameworks, J. Appl. Math. Mech. 49 (1985). https://doi.org/10.1016/0021-8928(85)90011-5

[20] A. V. Chentsov, D.S. Lisovenko, Experimental study of auxetic behavior of cellular structure, J. Phys. Conf. Ser. 991 (2018). https://doi.org/10.1088/1742-6596/991/1/012017

[21] D. Li, L. Dong, R.S. Lakes, A unit cell structure with tunable Poisson's ratio from positive to negative, Mater. Lett. 164 (2016). https://doi.org/10.1016/j.matlet.2015.11.037

[22] Y. Schneider, V. Guski, S. Schmauder, J. Kadkhodapour, J. Hufert, A. Grebhardt, C. Bonten, Deformation Behavior Investigation of Auxetic Structure Made of Poly(butylene adipate-co-terephthalate) Biopolymers Using Finite Element Method, Polymers (Basel). 15 (2023). https://doi.org/10.3390/polym15071792

[23] H. Cho, D. Seo, D.N. Kim, Mechanics of auxetic materials, in: Handb. Mech. Mater., 2019.

https://doi.org/10.1007/978-981-10-6884-3_25

[24] A. Joseph, V. Mahesh, D. Harursampath, On the application of additive manufacturing methods for auxetic structures: a review, Adv. Manuf. 9 (2021). https://doi.org/10.1007/s40436-021-00357-y

[25] S. Hou, T. Li, Z. Jia, L. Wang, Mechanical properties of sandwich composites with 3d-printed auxetic and non-auxetic lattice cores under low velocity impact, Mater. Des. 160 (2018). https://doi.org/10.1016/j.matdes.2018.11.002

[26] L.J. Gibson, M.F. Ashby, Cellular solids: Structure and properties, second edition, 2014.

[27] ASTM, ASTM C365-03: Standard test method for flatwise compressive properties of sandwich cores, Annu. B. ASTM Stand. (2008).

[28] O. Tolochyna, N. Zgalat-Lozynska, Y. Podrezov, D. Verbylo, O. Tolochyn, O. Zgalat-Lozynskyy, The role of flexible polymer composite materials properties in energy absorption of three-dimensional auxetic lattice structures, Mater. Today Commun. 37 (2023) 107370. https://doi.org/10.1016/j.mtcomm.2023.107370